International Journal of Chemical Studies

P-ISSN: 2349–8528
E-ISSN: 2321–4902
www.chemijournal.com
IJCS 2022; 10(5): 77-85

Received: 02-06-2022
Accepted: 06-07-2022

Ishwar Chand Balaee
Department of Chemistry, University of Rajasthan, Jaipur, Rajasthan, India

Vinayak Gupta
Department of Chemistry, University of Rajasthan, Jaipur, Rajasthan, India

Rekha Sharma
Department of Chemistry, University of Rajasthan, Jaipur, Rajasthan, India

Sarita Varshney
Department of Chemistry, University of Rajasthan, Jaipur, Rajasthan, India

Corresponding Author:
Ishwar Chand Balaee
Department of Chemistry, University of Rajasthan, Jaipur, Rajasthan, India

Electrochemical studies of Cu (II) complex of a novel Schiff base derived from sulfa drug

Ishwar Chand Balaee, Vinayak Gupta, Rekha Sharma and Sarita Varshney

Abstract
Cu (II) complex of novel Schiff base ligand derived from 2-hydroxy-2-methylpropiophenone and sulphamethazine sulpha drugs has been synthesized and characterized by various experimental and theoretical tools. The electrochemical behavior of sulpha drugs-Schiff base and its copper (II) Complex at a glassy carbon electrode were examined in the BR universal buffer and phosphate buffer of various pH levels (5.0-8.2) containing 10^{-3} mM examined compounds in various solvents. The cyclic voltammograms of the Schiff base ligand exhibited an irreversible diffusion-controlled cathodic step within the all pH range and the Cu (II) complex displayed a quasi-reversible redox process due to Cu (II)/Cu (I) process. The effects of solvent, buffer, sweep rate and pH are also studied on CV variables. Kinetic parameters like as charge transfer coefficient (α_n), diffusion coefficient ($D_0^{1/2}$) and rate constant (*k°f,h)* are also calculated from cyclic voltammograms.

Keywords: 2-Hydroxy-2-methylpropiophenone, Sulphamethazine, Cyclic voltammetry and Schiff base

Introduction
A large number of Schiff bases and their complexes have been studied for their interesting and important properties e.g. their ability to reversibly bind oxygen [1], catalytic activity in hydrogenation of olefins and transfer of an amino group [2], photochromic properties [3], and complexing ability towards some toxic metals [4]. Sulpha drugs constitute an important class of therapeutic agents in current medical science [5]. Sulpha drugs are the derivatives of sulfonamides and it is the basic functional group in all of these drugs. The sulfonamides are synthetic bacteriostatic antibiotics with a wide spectrum against various bacteria and fungi. Sulfonamides inhibit the multiplication of bacteria by acting as competitive inhibitors of p-aminobenzoic acid in the folic acid metabolism cycle [6-7]. Bacterial sensitivity is the same for the various sulfonamides, and resistance to one sulfonamide indicates resistance to all. The number of Schiff bases that are prepared from sulpha drugs and their metal complex shows a wide range of biological activities such as antibacterial, antifungal, anticonvulsant, antimalarial, and anticancer [8-12].
Cyclic voltammetry (CV) gives information about the thermodynamics of redox processes and the kinetics of heterogeneous electron–transfer reactions and coupled chemical reactions [13]. The characteristic shapes of the cyclic voltammograms and unequivocal position of potential wave exhibited electrochemical behavior of redox systems. The peak parameters for a particular process may depend on the scan rate, the concentration of the experimental solution, and the nature of the electrode [14-16]. In this paper, we are reporting synthesis, spectral analysis, and electrochemical behavior of such type of ligand and its Cu (II) complex.

Experimental section
Preparation of Schiff base ligand (HMPSMA)
All of the chemicals and solvents employed in synthesis were of extra pure grade and used as received without further purification. 2-hydroxy-2-methylpropiophenone and sulphamethazine were obtained from Sigma Aldrich. 30 ml Methanolic solution of 2-hydroxy-2-methyl propiophenone (0.757 ml) was added to a hot methanol-acetone solution of sulphamethazine (1.391gm) in equimolar ratio and the resulting solution was vigorously stirred and refluxed for 4-5 hours at 60-70°C and then left overnight in the refrigerator, the solid crude product obtained was filtered, washed with distilled water then ethanol.

The final product was recrystallized by ethanol then pale yellow crystals of new Schiff base are obtained with a good yield (68%). shown as fig.1.

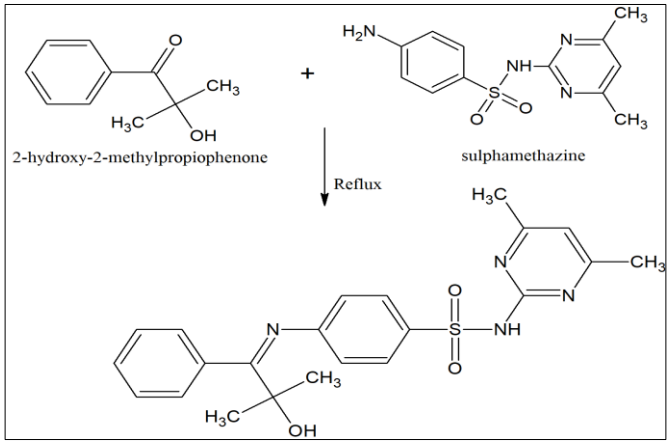

Fig 1: Synthesis of HMPSMA ligand

Synthesis of Cu (II) complex of HMPSMA

To synthesize Cu (II) complex, the acetone solution of prepared Schiff base ligand (2.0 mmol) was added drop wise to a solution of $Cu(AcO)_2.H_2O$ (1.0 mmol) dissolved in methanol, and all the contents were stirred with a magnetic needle on a magnetic stirrer for about 1 hour. The resulting mixture was then refluxed for 3-4 hours. The complex formed was filtered, recrystallized, and washed with ethanol; the excess solvent was removed under reduced pressure. The black solid crystals were obtained with a good yield.

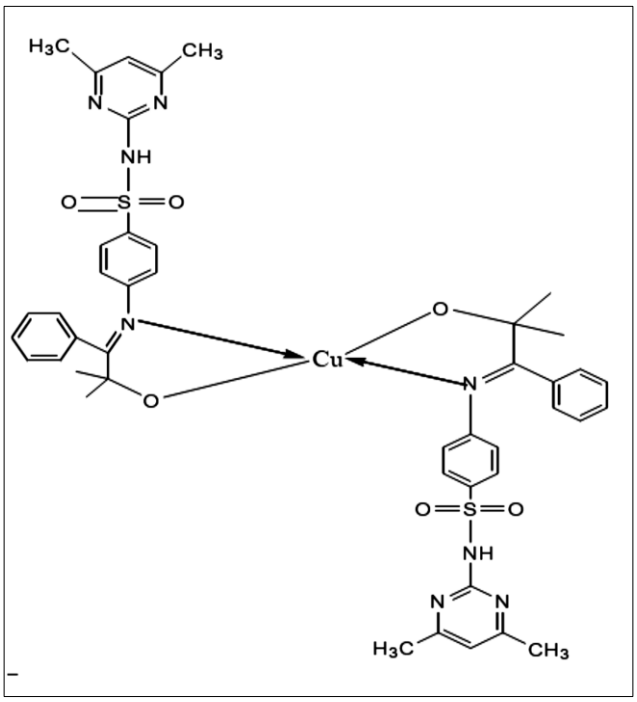

Fig 2: Proposed structure of 2-hydroxy-2 methyl propiophenone sulphamethazine copper (II) complex

Results and discussion

Table 1: Micro analytical data of Schiff base and its Cu (II) complex

S. No.	Composition of ligand/complex	colour	Yield (%)	M. Wt.	Melting Point	Elemental Analysis (%): found (Cal)			
						C	H	N	Cu
1.	C22H24N4O3S(L)	Pale yellow	68	424.48	165 °C	62.24 (62.30)	5.70 (5.39)	13.20 (13.26)	
2.	[CuL2]	black	73	910.49	187 °C	58.04 (58.40)	5.09 (5.23)	12.31 (12.51)	6.98 (6.92)

Infrared studies

The infra-red spectra of HMPSM ligand and their Cu (II) complex were recorded on KBr pellets in the range 4000-450 cm^{-1} on an FT-IR spectrometer (Schimadzu). Ligand showed a strong band at 1630-1636 cm-1 that was attributed to azomethine υ(C=N) [17]. The absence of bands near 1723 cm^{-1} and 3600 cm^{-1} due to carbonyl stretching and NH_2 str. respectively indicates the condensation of reaction reactants. The bands appeared at 1228-1363cm^{-1}and1130-1160 cm^{-1}due to asymmetric and symmetric stretching of SO_2 respectively in spectra. Other additional band at 1400-1600 cm^{-1}, 980 cm^{-1} and 677 cm^{-1} are assigned to C=C(Ar), S-N, C-S stretching

vibration respectively. In comparison to the HMPSMA ligand spectra with Cu (II) complex, then it was found that the band of υ(C=N) in the region of 1630-1636 cm^{-1}show shifting towards lower wavenumber, indicating coordination of the nitrogen atom of ligand to Cu (II) ion. The broad and strong band due to υ(OH) 3200-3450 cm^{-1} in ligand spectra, disappear in the complex formation, showing oxygen coordination to metal ion by deprotonation. The appearance of new bands in regions 440-462 cm^{-1} and 515-565 cm^{-1} assignable to υM-O and υM-N respectively attributed to the bonding of metal ions to oxygen and nitrogen atoms.

Cyclic voltammetric studies

The electrochemical response of HMPSMA Schiff base ligand was studied by recording the cyclic voltammograms at a wide range of scan rates from 0.05 and 0.25 V/s and investigated in the potential range +8.0V to -1.6V and in pH 5.0 to 8.2 with phosphate buffer and BR buffer employing cyclic voltammetry Cyclic voltammograms measurements were performed using computerized Constant Current Source (Cyclic Voltammetry System).

The electrode assembly used for this experiment was incorporated with a micro-electrochemical cell with a three-electrode configuration system comprising a glassy carbon electrode the working electrode, an Ag/AgCl/KCl reference electrode, and a platinum wire auxiliary electrode. All cyclic voltammograms of ligand were obtained, exhibiting one irreversible reduction peak; this may be attributed to the reduction of the azomethine group by the two-electron process. Representative Voltammograms are shown in Figures 3, 4, 5 and 6. With the help of cyclic voltammograms, kinetic parameters such as charge transfer coefficient (α_n), diffusion coefficient ($D_0^{1/2}$) rate constant($k°f,h$)have been evaluated for irreversible and diffusion controlled reduction using the following equations [18-20] (1-3) and reported in table (2-5).

$$\left|E_p - E_{p/2}\right| = \frac{1.857RT}{\alpha_n F} = \left(\frac{47.7}{\alpha_n}\right) mV \quad (1)$$

$$I_P = 3.01\times10^5 n(\alpha_n)^{1/2} A C D_0^{1/2} v^{1/2} \quad (2)$$

$$E_P = -\frac{RT}{\alpha_n F}\left[0.78 + \ln\left(\frac{D_0^{1/2}}{k^\circ_{f,h}}\right) + \ln\left(\frac{\alpha_n F v}{RT}\right)^{1/2}\right] \quad (3)$$

Table 2: Effect of sweep rate on voltammetric parameters of HMPSMA ligand in acetone phosphate buffer at different pH (5, 7, 8.2) (fig.3 A, B, C)

pH	*v* (mVs^{-1})	*Epc* (mV)	*Ipc* (µA)	*Ep/2* (mV)	*Ipc/* $v^{1/2}$	α_n	$D_0^{1/2}$ (cm^2s^{-1})	*k°f,h* ($cm.s^{-1}$)
5	50	-812	22.34	-732	3.159353	0.59625	25.75497534	3.92E-10
	100	-840	27.7	-754	2.77	0.554651	23.41245593	9.90E-10
	150	-852	32.8	-770	2.678109	0.581707	22.10309644	3.69E-10
	200	-860	42.6	-778	3.012275	0.581707	24.86105221	3.99E-10
	250	-869	49.4	-786	3.12433	0.574699	25.94262805	4.79E-10
7	50	-838	27.1	-755	3.832519	0.574699	31.82301424	5.26E-10
	100	-850	31.4	-763	3.14	0.548276	26.69360641	1.12E-09
	150	-872	44.4	-785	3.625245	0.548276	30.81874469	9.87E-10
	200	-885	50.3	-792	3.556747	0.512903	31.2616891	2.87E-09
	250	-896	60.8	-813	3.84533	0.574699	31.92938836	3.22E-10
8.2	50	-846	34.1	-767	4.822468	0.603797	39.06617585	2.12E-10
	100	-865	47.7	-777	4.77	0.542045	40.78286139	1.52E-09
	150	-884	60.1	-792	4.907144	0.518478	42.89836443	2.88E-09
	200	-899	69.2	-812	4.893179	0.548276	41.59764087	8.64E-10
	250	-912	74.8	-828	4.730767	0.567857	39.51747751	3.53E-10

Table 3: Effect of sweep rate on voltammetric parameters of HMPSMA ligand in acetone- BR buffer at different pH (5, 7, 8.2) (fig.4 A, B, C)

pH	*v* mVs^{-1}	*Epc* (mV)	*Ipc* (µA)	*Ep/2* (mV)	*Ipc/* $v^{1/2}$	α_n	$D_0^{1/2}$ (cm^2s^{-1})	*k°f,h* ($cm.s^{-1}$)
5	50	-844	30.67	-759	4.337393	0.561176	36.4465324	8.11E-10
	100	-854	32.6	-765	3.26	0.535955	28.03048302	1.60E-09
	150	-874	30.2	-788	2.46582	0.554651	20.84147814	5.18E-10
	200	-886	35.2	-799	2.489016	0.548276	21.15949362	5.80E-10
	250	-897	39.12	-811	2.474166	0.554651	20.91202289	4.08E-10
7	50	-865	34.4	-775	4.864895	0.53	42.06420384	1.64E-09
	100	-879	39.8	-796	3.98	0.574699	33.04761302	3.08E-10
	150	-894	49.5	-817	4.041658	0.619481	32.32383716	5.77E-11
	200	-910	46.5	-834	3.288047	0.627632	26.12538682	2.76E-11
	250	-925	58.9	-845	3.725163	0.59625	30.3674456	7.50E-11
8.2	50	-872	41.2	-794	5.82656	0.611538	46.90050224	1.07E-10
	100	-890	57.31	-813	5.731	0.619481	45.83463205	7.35E-11
	150	-910	63.9	-829	5.217413	0.588889	42.79723547	1.50E-10
	200	-922	70.64	-843	4.995002	0.603797	40.46385135	7.35E-11
	250	-942	73.8	-859	4.667522	0.574699	38.75639575	1.40E-10

Table 4: Effect of sweep rate on voltammetric parameters of HMPSMA ligand in DMF phosphate buffer at different pH (5, 7, 8.2) (fig.5 A, B, C)

pH	*v* (mVs^{-1})	*Epc* (mV)	*Ipc* (µA)	*Ep/2* (mV)	*Ipc/* $v^{1/2}$	α_n	$D_0^{1/2}$ (cm^2s^{-1})	*k°f,h* ($cm.s^{-1}$)
5	50	-929	26.66	-851	3.761	0.61154	30.28038	1.77E-11
	100	-961	37.90	-869	3.790	0.51848	33.13221	3.83E-10
	150	-983	27.00	-889	3.830	0.50745	33.91039	4.65E-10
	200	-995	53.40	-882	3.775	0.42212	36.58352	1.14E-08
	250	-1006	58.90	-893	3.725	0.44579	35.12023	4.14E-09
7	50	-952	33.70	-872	4.765	0.59625	38.85151	2.28E-11
	100	-970	41.00	-880	4.100	0.5300	35.45056	2.17E-10
	150	-993	47.90	-891	3.911	0.46765	36.00034	1.81E-09
	200	-1010	62.10	-899	4.391	0.42973	42.16537	7.66E-09
	250	-1030	68.40	-912	4.320	0.40424	42.82956	1.68E-08
8.2	50	-957	37.6	-850	5.317443	0.445794	50.13173206	6.20E-09
	100	-982	46.1	-870	4.61	0.425893	44.46598477	1.05E-08
	150	-1001	59.4	-890	4.84999	0.42973	46.5715061	8.54E-09
	200	-1020	85.2	-905	6.02455	0.414783	58.88321243	1.61E-08
	250	-1035	92.9	-920	5.875512	0.414783	57.42653439	1.38E-08

Table 5: Effect of sweep rate on voltammetric parameters of HMPSMA ligand in Methanol- phosphate buffer at different pH (5, 7, 8.2) (fig.6 A, B, C)

pH	*v* (mVs^{-1})	*Epc* (mV)	*Ipc* (µA)	*Ep/2* (mV)	*Ipc/* $v^{1/2}$	α_n	$D_0^{1/2}$ (cm^2s^{-1})	*k°f,h* ($cm.s^{-1}$)
5	50	-875	29.3	-780	4.143646	0.502105	36.80971026	2.95E-09
	100	-910	32.2	-810	3.22	0.477	29.34768506	3.98E-09
	150	-930	42.1	-830	3.437451	0.477	31.32957074	3.58E-09
	200	-955	50.2	-856	3.549676	0.481818	32.19024594	2.25E-09
	250	-985	53.4	-870	3.377313	0.414783	33.00943958	1.78E-08
7	50	-915	37.4	-808	5.289159	0.445794	49.86507391	1.28E-08
	100	-937	42.4	-830	4.24	0.445794	39.97382655	9.90E-09
	150	-967	51.3	-858	4.188627	0.437615	39.85684913	9.68E-09
	200	-990	53.5	-877	3.783021	0.422124	36.65185706	1.24E-08
	250	-1015	56.4	-898	3.567049	0.407692	35.16576008	1.53E-08
8.2	50	-927	41.22	-837	5.829388	0.53	50.40367681	5.48E-10
	100	-971	49.4	-858	4.94	0.422124	47.86126233	1.56E-08
	150	-988	52.3	-876	4.270277	0.425893	41.18917078	1.08E-08
	200	-1010	58.8	-898	4.157788	0.425893	40.10415017	8.46E-09
	250	-1025	66.4	-910	4.199505	0.414783	41.04544547	1.16E-08

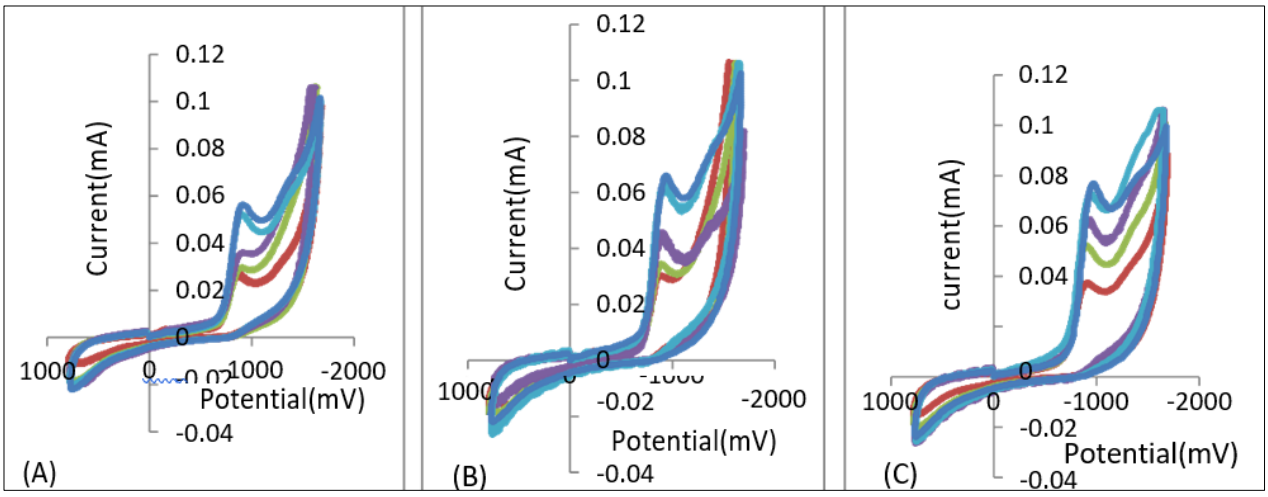

Fig 3: Cyclic voltammogram of 1.0 mM HMPSMA ligand in acetone -phosphate buffer at (A) 5.0 pH (B) 7.0 pH (C) 8.2 pH

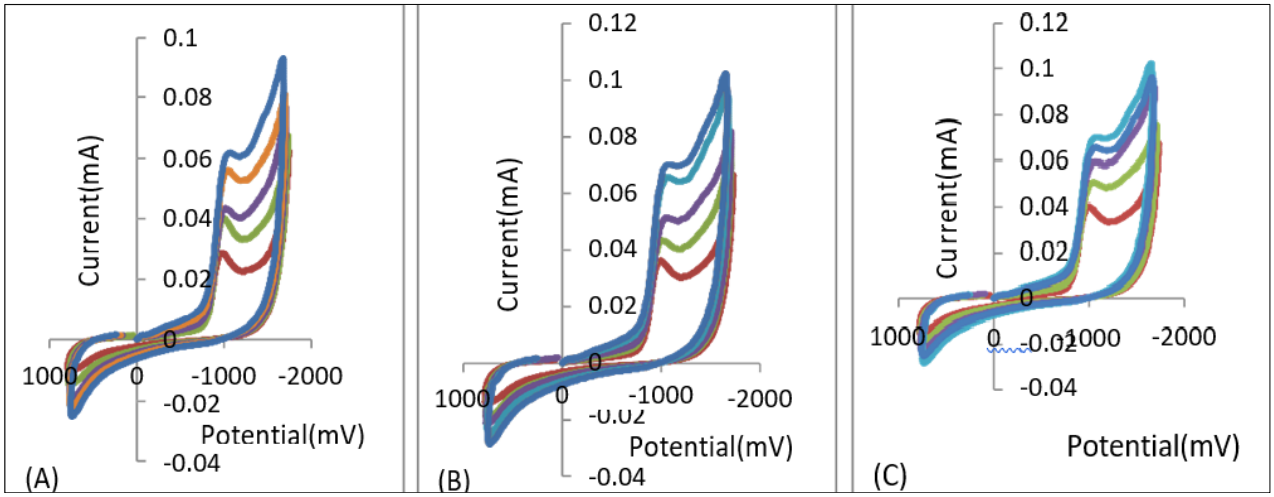

Fig 4: Cyclic voltammogram of 1.0 mM HMPSMA ligand in acetone -BR buffer at (A) 5.0 pH (B) 7.0 pH (C) 8.2pH

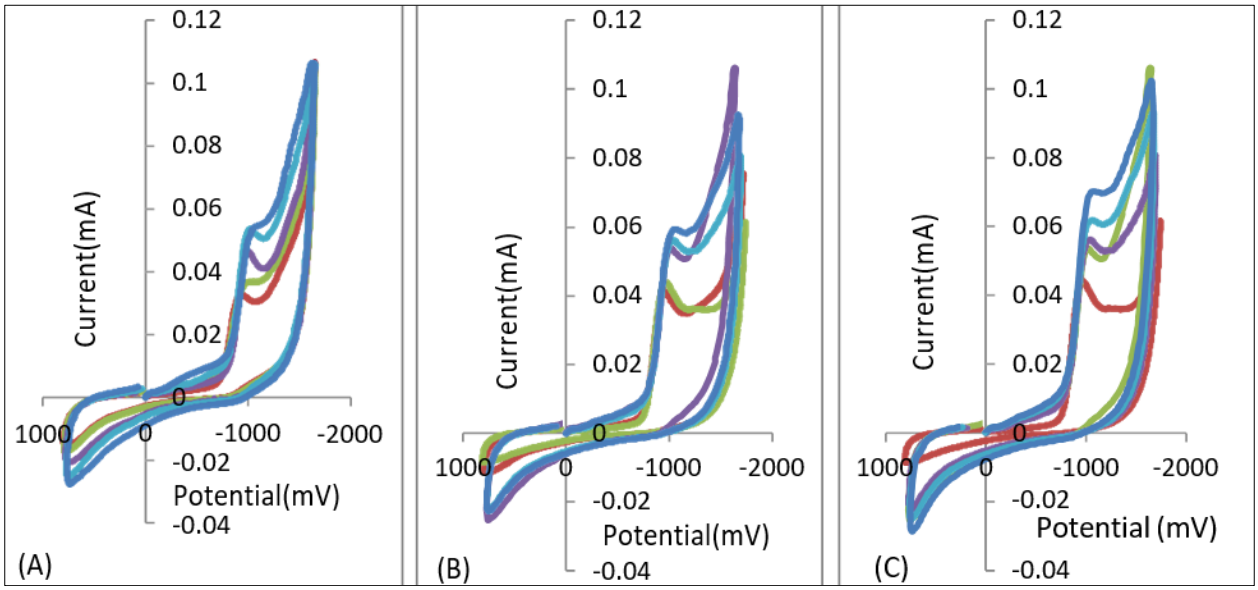

Fig 5: Cyclic voltammogram of 1.0 mM HMPSMA ligand in DMF -phosphate buffer at (A) 5.0 pH (B) 7.0 pH (C) 8.2pH

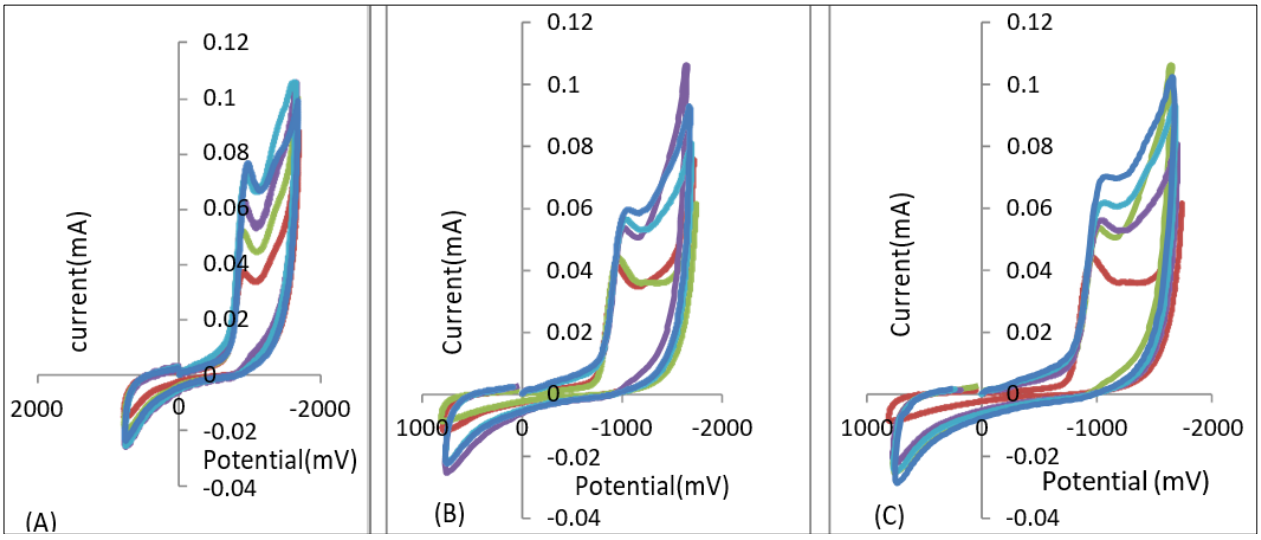

Fig 6: Cyclic voltammogram of 1.0 mM HMPSMA ligand in methanol -phosphate buffer at (A) 5.0 pH (B) 7.0 pH (C) 8.2pH

The effect of various factors (pH, sweep rates, solvent of experimental solution and buffer solution) on cyclic voltammograms

The cyclic voltammograms of azomethine ligand (HMPSMA) show one irreversible reduction peak at considered scan rates. The appearance of the peak on the cathodic side at -812mV to -1035mVmay most probably be due to the reduction of the –C=N–(azomethine) group of the adsorbed molecule [21]. Cyclic voltammograms parameters are affected by various factors as follows.

The pH effect on the electrochemical process of ligand has been investigated. The studied pH are 5.0, 7.0, and 8.2. (fig.3, 4, 5, and 6) .All cyclic voltammograms demonstrate that the parameters of cathodic peak change with pH. At higher pH both cathodic peak potential and cathodic peak current values are high and get less at lower pH. (fig.7,8) Moreover, the cathodic peak is shifted towards a negative potential direction with increasing pH. This confirms the participation of protons in the electrode reduction process. The reduction is easier at low pH in comparison to higher pH. It confirmed the formation of an easily reducible protonated intermediate during the reduction [22] (table 1, 2, 3, 4).

The cyclic voltammogram parameters like Epc, Ipc, and Ep/2 are affected by changing the scan rate. During cyclic voltammetry study, when the scan rate is applied from 50 to 250 mVs-1 at constant pH and concentration, the reduction signals significantly shift to more negative potentials with faster scan rates. This establishes the electrochemical process was irreversible. (fig.3, 4, 5, and 6)

On drawing a plot between the peak current (Ipc) which is obtained from the cyclic voltammograms and the square root of scan rate ($v^{1/2}$), a linear relationship is obtained in it, which shows the irreversible nature of the electrochemical process. (fig.7, 8) Peak current increases with the increase of the square root of the scan rates. From these observations, it is concluded that the electrode process is diffusion-controlled [23-26].

The properties of a solvent also affect the electrochemical behavior of an electro active species. For comparative study of the electrochemical behavior of ligand, cyclic voltammograms of HMPSMA were recorded in three distinct solvents like acetone, CH3OH, and DMF media with phosphate buffer. It showed that the negative peak potential value is maximum (-1035at 250 mVs^{-1} at 8.2 pH) in aprotic solvent DMF and minimum (-912 at 250 mVs-1 at 8.2 pH) in acetone solvent (fig.9). The order of negative peak potential value in the present study is DMF-phosphate >CH_3OH-phosphate>CH_3COCH_3- phosphate buffer. This trend is similar to the trend in viscosity, and the dielectric constant of solvents [27].

The effect of buffer medium (BR buffer and Phosphate buffer) on the electrochemical process of HMPSMA was also studied. To observe this effect, the cyclic voltammograms of the ligand was taken in phosphate buffer and BR buffer with acetone solvent at 50-250 mV/s sweep rate and at three distinct pH values (5, 7, 8.2) .This establishes that the peak potential shifts towards more negative potentials with a buffer solution of less polarity.(fig.10) The reduction potential value in acetone - phosphate buffer is reported to vary from -812mV to -912 mV at 50 to 250 mVs^{-1} scan rates at three distinct pH values. While in acetone – BR buffer, Epc values varies from -844mV to -942 mV at 50- 250mVs-1, it may be due to low ionized components in BR buffer [23].

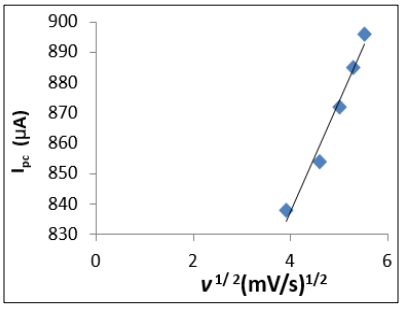

Fig 7: Ipc vs v1/2 for 1mM HMPSMA in acetone phosphate buffer at pH 7.0

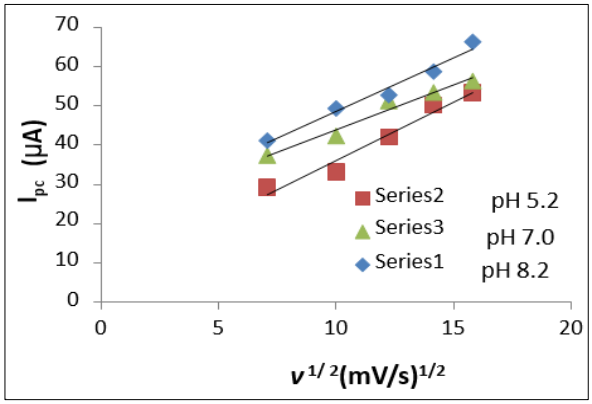

Fig 8: IpC v/s v 1/2 in methanol-phosphate buffer of HMPSMA

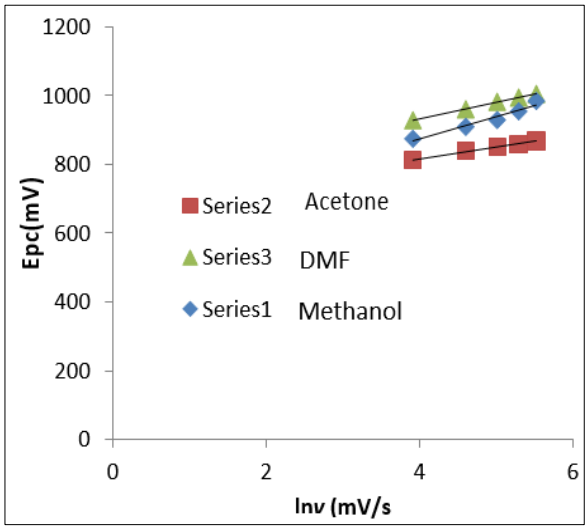

Fig 9: Epc v/s lnv for HMPSMA in acetone, DMF and methanol solvents at pH 7.0

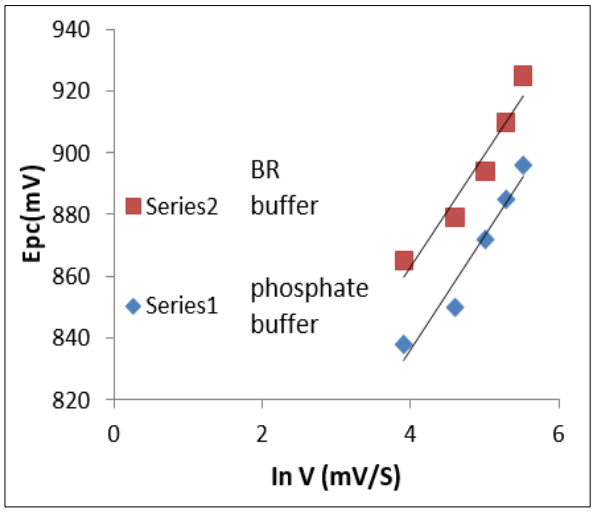

Fig 10: Epc v/s lnv for HMPSMA in acetone solvent at pH 7.0 in different buffer

Electrochemical studies of Cu (II) complex

For observing the effect of concentration of copper (II) complex and scan rates on electrochemical parameters, three experimental solutions possessing the concentration of copper (II) complex 1-3 mM in DMF solvent containing sodium perchlorate as supporting electrolyte were prepared. Cyclic voltammograms were recorded on glassy carbon electrode within the potential range +700 to -1200mV with several scan rates changing from 100 to 300 mVs-1 employing cyclic

voltammetry techniques (fig.11-14). In the forward scan cathodic peaks ranging from about -510mV to -585mV, and in the reverse scan, the anodic peaks ranging from about -220mV to -104mV are observed for 1mM Cu (II) complex. All the cyclic voltammograms show a well-defined quasireversible [28] and one-electron transfer redox reaction for the redox couple Cu (II)/Cu (I). The possible mechanism of the redox reaction for the all cyclic voltammograms is as follows. For reduction Cu (II) +1e-=Cu (I) and for oxidation Cu (I) -1e- = Cu (II). Cyclic voltammetric data are compiled in table 6.0.

Table 6: Cyclic voltammograms data for the effect of scan rate and concentrations on CV parameters for 1.0 to 3.0 mM Cu (II) complex in DMF with NaClO4 at glassy carbon electrode.

Complex Conc.	*v* mVs-1	*Epc* mV	*Epa* mV	*ΔEp* mV	$E^{1/2}$ mV	*Ipc* µA	*Ipa* µA	*Ipa/Ipc*	*Ipc*/ $v^{1/2}$
1Mm	100	-510	-220	290	-360	8.3	5.4	0.650602	0.83
	150	-520	-170	350	-340	13.6	8.4	0.617647	1.110435
	200	-540	-135	405	-380	15.4	9.7	0.62987	1.088944
	250	-570	-115	455	390	19.2	11.7	0.609375	1.214315
	300	-585	-104	481	-398	24.7	15.3	0.619433	1.426055
2Mm	100	-489	-139	350	-351	13.22	10.3	0.779123	1.322
	150	-530	-130	400	-360	18.8	12.1	0.643617	1.535069
	200	-550	-120	430	-390	24.3	13.5	0.555556	1.718273
	250	-590	-100	490	-395	29.6	16.4	0.554054	1.872078
	300	-600	-90	510	-410	31.1	17.9	0.69112	1.795560
3Mm	100	-560	-10	550	-350	24.7	15.6	0.631579	2.47
	150	-590	20	610	-385	26.3	18.67	0.709886	2.147386
	200	-620	60	680	-410	36.2	21.6	0.596685	2.559727
	250	-630	90	720	-430	40	23.3	0.5825	2.529822
	300	-650	110	760	450	41.1	23.53	0.572506	2.37291

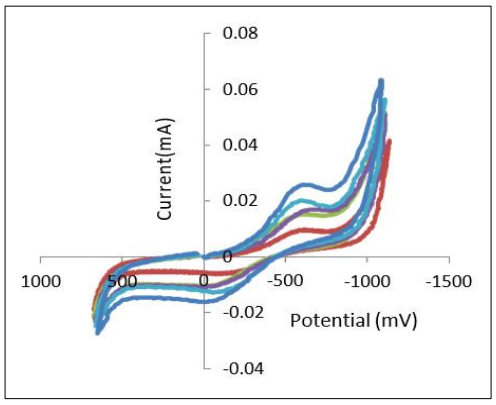

Fig 11: Cyclic voltammograms response of 1.0 mM Cu (II) in DMF at 100,150,200,250,300 mVs^{-1} scan rates

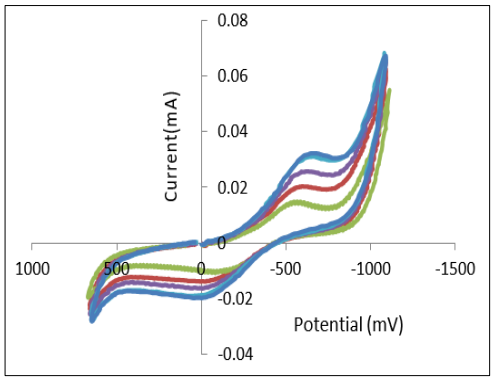

Fig 12: Cyclic voltammograms response of 2.0 mM Cu (II) in DMF at 100,150,200,250,300 mVs^{-1} scan rates

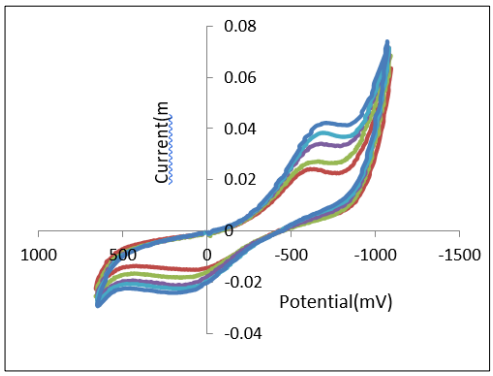

Fig 13: Cyclic voltammograms response of 3.0 mM Cu (II) in DMF at 100,150,200,250,300 mVs^{-1} scan rates

The adsorption behaviour of 1.0mM the Cu(II) complex was studied by recording the cyclic voltammogram (figure14) at a scan rate of 0.2V/s with double scan (number of cycles=2). The peaks are observed almost in the same potential regions in each cycles suggest that the complex molecules are not adsorbed on electrode surface

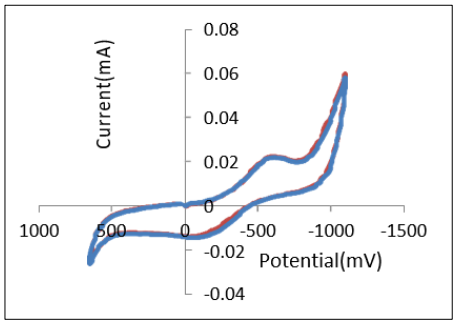

Fig 14: Cyclic voltammograms response of 1.0 mM Cu (II) in DMF at, 200, mVs^{-1} scan rates with double scan

Effect of scan rate and concentration on cyclic voltammetric measurements of Cu (II) complex

The observed data of potential current curves reveals that both cathodic and anodic peak current linearly increased with the increase of scan rate and concentration (fig. 15, 16). The reduction peak potential shifted towards the negative direction in the cathodic region and the anodic peak potential shifted slightly towards positive potential with the increase in scan rates and concentration. In all the cases the cathodic peak current (Ipc) is proportional to the square root of the scan rate ($v^{1/2}$) (fig.15), which confirmed that under these conditions, the redox process is diffusion controlled [29-30]. The cathodic and anodic peak potential difference (ΔEp) is in the range 290mVto 481mV for a 1.0mM complex, it is though being much larger than the theoretical value (0.059 V) for a redox reversible one-electron process, which suggests that the redox behavior of complex corresponds to a quasi-reversible one electron charge transfer process under the non-aqueous experimental condition of the system. The separation of the two signals increases with faster scan rates. The ratio of oxidation peak current to its corresponding reduction peak current (Ipa/Ipc) is about 0.65 to 0.61 for a 1.0mM complex. This ratio is less than unity (Ipa/Ipc<1), further confirming the quasi-reversible redox system [31].

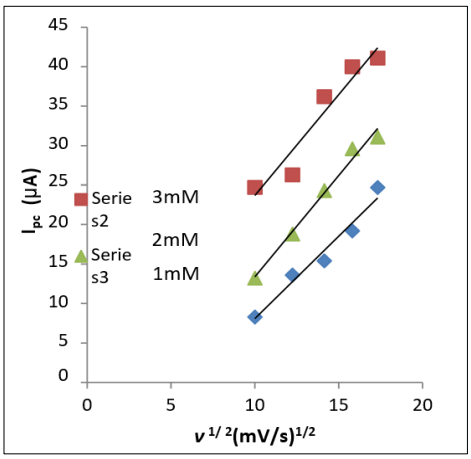

Fig 15: Plot of peak current (Ipc) v/s square root of the sweep rate ($v^{1/2}$) for1.0, 2.0, 3.0 mM Cu (II) complex in DMF solvent with sodium perchlorate as supporting electrolyte

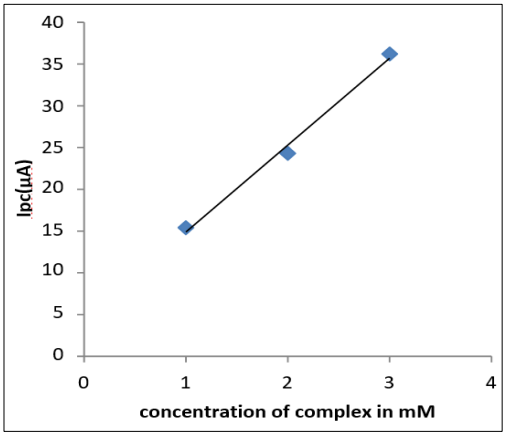

Fig 16: A plot Ipc v/s concentration of complex

Acknowledgement

The authors are grateful to the Head, Department of Chemistry, University of Rajasthan, Jaipur for providing research facilities

References

1. Shukla SN, Gaur P, Raidas ML, Bagri SS. Synthesis, spectroscopic characterization, DFT, oxygen binding, antioxidant activity on Fe (III), Co (II) and Ni (II) complexes with a tetradentate ONNO donor Schiff base ligand. Journal of the Serbian Chemical Society. 2021;86(10):941-54.
2. Alexander S, Udayakumar V, Gayathri V. Hydrogenation of olefins by polymer-bound palladium (II) Schiff base catalyst, J Mol Catal A Chem. 2009;314(1-2):21-27.
3. Matozzo P, Colombo A, Dragonetti C, Righetto S, Roberto D, Biagini P, *et al*. A Chiral bis (salicylaldiminato) zinc (II) complex with second-order nonlinear optical and luminescent properties in solution. in organics. 2020;8(25):1-11.
4. Vinusha HM, Kollur SP, Revanasiddappa HD, Ramu R, Shirahatti PS, Prasad MN, *et al*. Preparation, spectral characterization and biological applications of Schiff base ligand and its transition metal complexes. Results Chem. 2019;1:100012.
5. Ali A, Reddy GSKK, Cao H. Discovery of HIV-1 protease inhibitors with picomolar affinities incorporating N-aryl oxazolidinone-5- carboxamides as novel p2 ligands. J. Med. Chem. 2006;49(25):7342-7356.
6. Capasso C, Supuran CT. Sulfa and trimethoprim-like drugs–antimetabolites acting as carbonic anhydrase, dihydropteroate synthase and dihydrofolate reductase inhibitors. J. Enzyme Inhib. Med. Chem. 2014;29(3):379-387.
7. Azzam RA, Elsayed RE, Elgemeie GH. Design, synthesis, and antimicrobial evaluation of a new series of n-sulfonamide 2-pyridones as dual inhibitors of DAPS and DHFR enzymes. ACS Omega. 2020;5(18):10401-10414.
8. Kuate M, Conde MA, Mainsah EN, Paboudam AG, Tchieno FMM, Ketchemen KIY, *et al*. Synthesis, characterization, cyclic voltammetry and biological studies of Co(II), Ni(II), and Cu(II) complexes of a tridentate schiff base, 1-((e)-(2-mercaptophenylimino) methyl) naphthalen-2-ol (H2L1); J. Chem. 2020;10:21.
9. Borase JN, Mahale RG, Rajput SS, Shirsath DS. Design, synthesis and biological evaluation of heterocyclic methyl substituted pyridine Schiff base transition metal complexes. SN Appl. Sci. 2021;3(2):197.
10. Najm S, Naureen H, Sultana K, Anwar F, Khan MM, Nadeem H, *et al*. Schiff-based metal complexes of lamotrigine: design, synthesis, characterization and biological evaluation, ACS Omega. 2021;6(1):7719-7730.
11. Hubin TJ, Amoyaw P, Roewe KD, Simpson NC, Maples RD, Freeman TNC, *et al*. Synthesis and antimalarial activity of metal complexes of crossbridged tetraazamacrocyclic ligands. Bioorg Med Chem. 2014;22(13):3239-3244.
12. Mbugua N, Sibuyi NRS, Njenga LW, Odhiambo RA, Wandiga SO, Meyer M, *et al*. New palladium (II) and platinum (II) complexes based on pyrrole Schiff bases: synthesis, characterization, X-ray structure, and anti-cancer activities. ACS Omega. 2020;5(25):14942-14954.
13. Rupara J, Aleksic MM, Nikolic K, Nikolic MRP. Comparative electrochemical studies of kinetic and thermodynamic parameters of quinoxaline and brimonidine redox process; Electrochim. Acta. 2018;271:220-231.

14. Kumawat GL, Choudhary P, Varshney AK, Varshney S. Cyclic voltammetric studies of biologically active azomethine2'-hydroxyacetophenone sulfamethoxazole Orient. J. Chem. 2019;35(3):1117-1124.
15. Choudhary P, Kumawat GL, Sharma R, Varshney S. Synthesis, electrochemical and antimicrobial activity of Schiff base and its nickel (II) complex Int. J. Pharm. Sci. 2018;9(11):4601-4609.
16. Randviir EP. A cross examination of electron transfer rate constants for carbon screen-printed electrodes using electrochemical impedance spectroscopy and cyclic voltammetry Electrochim. Acta. 2018;286:179-186.
17. Ommenya FK, Nyawade EA, Andala DM, Kinyua J. Synthesis, characterization and antibacterial activity of Schiff base, 4-chloro-2-{(e)-[(4- fluorophenyl)imino] methyl}phenol metal (II) complexes J. Chem; c2020.
18. Parajoan-Costa BS, González-Baro AC, Baran EJZ. Electrochemical and spectroscopic behaviour of bis(2-mercaptopyridine-N-oxide) oxovanadium (IV). Anorg. Allg. Chem. 2002;628(6):1419-1424.
19. Electrochemical methods, fundamentals and applications; A.J.Bar and L.R. Faulkner, (Wiley, New York), 2 1980.
20. Sharma P, Kumar A, Sharma M. Synthesis and electrochemical investigations on 2-phenyl-4-[4'-(3"-ethoxy) phenylazophenyl]-3-thioxo-3,4-dihydro-2H, 2, 4, 9, 10-tetraazaphenanthrene-1-one Indian J. Chem. 2006;45(4):872-876.
21. Abayneh A, Gebretsadik T, Tadesse S, Thomas M. Synthesis, spectroscopic, structural, characterization, conductivity and electrochemical studies of a Schiff base ligand and its copper complexes Adv. Chem. Eng. Sci. 2018;8(4):241-254.
22. Choudhary P, Sharma A, Varshney AK, Varshney S. Cyclic voltammetric reduction of amino acid ketimine and its Co (II) complex; J. Indian Chem. Soc. 2017;94:1-10.
23. Meena L, Choudhary P, Varshney AK, Varshney S. Electrochemical behaviour of 4-tertbutylcyclohexanone semicarbazone and its Co (II) complex; Port Electrochim. Acta. 2019;37(4):271-283.
24. Abbas SH, Murad DMA, Abbas HH. Spectral and cyclic voltammetry studies of chloro-salicyliden aniline and some of its complexes with Co (II) and Mn (II) J. Phys.: Conf. Ser. 2020;1660:012034.
25. Das R, Saxena A, Saxena S, Khan G. Electrochemical study of some Schiff base by cyclic voltammetry and its metal complex - DNA interaction study by UV-visible spectroscopy; J. Adv. Electrochem. 2015;1(1):19-24.
26. Gopinath SK, Pari M, Rudrannagari AM, Kattebasaveshwara IB, Halappa SK. Synthesis, characterization and electrochemical sensor based upon novel Schiff base metal complexes derived from the non-steroidal anti-inflammatory drug, flufenamic acid for the determination of uric acid and their biological applications; Biointerface Res. Appl. Chem. 2021;11(4):11390-11403.
27. Sahli R, Bahri J, Tapsoba I, Boujlel K, Raouafi N. Solvent effects on the electrochemical behavior of TAPD-based redox-responsive probes for cadmium (II); Int. J. Chem; c2014.
28. Bavane JN, Mohod RB. Synthesis, characterization and electrochemical studies of symmetrical Schiff base complexes of [1-(5 chloro-2- hydroxy-4-methyl- phenyl) ethanone-4-chloro (-3- trifluro methyl) aniline]; J. Pharm. Inno. 2018;7(1):149-152.
29. Wang J. Analytical Electrochemistry; Wiley-VCH, Inc; c1948.
30. Nicolson RS, Shain I. Simulation of the electrochemical behavior of multi-redox system, Anal. Chem. 1964;36:706.
31. Spectral and cyclic voltammetric studies on Cu(II)-Schiff base complex derived from anthracene-9(10H)- one; IOSR J. Appl. Chem. 2014;7(10):64-68.